COMPREHENSIVE SUMMARIES OF UPPSALA DISSERTATIONS FROM THE
FACULTY OF SCIENCE AND TECHNOLOGY 537

Friction and Contact Phenomena of Disc Brakes Related to Squeal

BY

MIKAEL ERIKSSON

ACTA UNIVERSITATIS UPSALIENSIS
UPPSALA 2000

ENCLOSED PAPERS

The thesis comprises the following papers:

Paper I — Mikael Eriksson, Filip Bergman and Staffan Jacobson, *Surface characterisation of brake pads after running under silent and squealing conditions*, Wear 232 (1999) 163-167.

Paper II — Filip Bergman, Mikael Eriksson and Staffan Jacobson *Influence of disc topography on generation of brake squeal*, Wear 225-229 (1999) 621-628.

Paper III — Mikael Eriksson, Filip Bergman and Staffan Jacobson *A study of initialisation and inhibition of disc brake squeal*, Accepted for publication in proceedings of Brakes 2000, Leeds, UK

Paper IV — Mikael Eriksson, Filip Bergman and Staffan Jacobson *On the nature of tribological contact in automotive brakes*, Submitted to Wear, Dec. 1999

Paper V — Mikael Eriksson, Anna Lundqvist and Staffan Jacobson *A study of the influence of humidity on the friction and squeal generation of automotive brake pads*, Submitted to Journal of Automobile Engineering, March 2000

Paper VI — Mikael Eriksson and Staffan Jacobson *Friction behaviour and squeal generation of disc brakes at low speeds*, Submitted to Journal of Automobile Engineering, March 2000

Paper VII — Mikael Eriksson, John Lord and Staffan Jacobson *Wear and contact conditions of brake pads - dynamical in-situ studies of pad on glass*, Accepted for publication in proceedings of Nordtrib 2000, Porvoo, Finland.

Paper VIII — Mikael Eriksson and Staffan Jacobson Tribological surfaces of organic brake pads, Submitted to Tribology International, March 2000

CONTENTS

1 INTRODUCTION

When Henry Ford introduced his model T in 1908, cars had been produced like he knew them for over 25 years, with a combustion engine in front of the passengers, four wheels and rear wheel drive. Even if the design was traditional, the model T was revolutionary. It was the first mass-produced car ever and with it, cars became more accessible to ordinary people.

No one knows if it is true that Henry Ford once said; “You can paint it any color, so long as it's black." [1]. Nevertheless, what is true, is that black was the only available colour on the model-T between 1914 and 1926. It is also true that the reason for this was that the black enamel was the fastest drying paint available at the moment. Production time could be reduced with a quick-drying paint and with it, also cost. This low price philosophy founded what would become the largest family company in the world, the Ford Motor Company.

The model T weighed 550 kg, had a 20-hp engine and a top speed of approximately 65 km/h see Fig 1. It was equipped with a band brake system, a cotton textile band wound around a drum inside the planetary gearbox. The cotton band was lubricated with the oil from the gearbox and in order to avoid over-heating, the driver was instructed to apply the brake in short intervals only.

Fig. 1. Ford model-T, the first mass-produced car in history. It was equipped with a cotton band brake, applied to a drum within the gearbox.
(Henry Ford Museum)

Eighty-three years later Mercedes-Benz reintroduced the 600 S-class (the name was also used in the 60's). Designed to be the best and most comfortable car in the world, it weighed over 2 tons, with a 400-hp engine and an electronically limited top speed of 250 km/h (for safety reasons). The maximum kinetic energy was now 54 times higher than 80 years earlier, putting enormous demands on the brake performance. The model–T's single band brake was replaced by four disc brakes and no one even thought about giving the driver special instructions on how to take care of the them. Nowadays, it is taken for granted that the brake systems should always work perfectly, despite careless users, extreme speeds and difficult environments.

On sports cars, the brake performance demands are sometimes even higher than on the Mercedes 600 S. For example, the Ferrari 550, one of the fastest cars on the market, has a top speed of 320 km/h. This results in a 40% higher maximum kinetic energy, as compared to the Mercedes.

1.1 Outline of the thesis

The aim of the work presented in this thesis has been to increase the understanding of the contact and friction phenomena in the brake pad and disc couple. This understanding is needed to analyse and ultimately solve the brake squeal problem. The thesis is mainly a review of the appended papers. In cases where the presented information is not found in the papers, the source is referred to using a number in square brackets [].

The work comprises a number of investigations correlated to the tribology of brake pad materials and squeal generation in brake systems. It is presented according to the following outline:

- First of all, we will start with a fundamental introduction to the friction and the contact between two rubbing surfaces. This is followed by a general description of the brake system and brake squeal testing.
- Chapter 2 comprises the main part of the thesis, describing the specific contact situation found between a brake pad and a disc.
- This description is followed by chapter 3, where the dynamical behaviour of this contact is discussed.
- Chapter 4 outlines a number of friction phenomena typical of brakes. These phenomena are correlated to the contact situation and to the generation of brake squeal.
- A summary of the thesis is found in Chapter 5.

1.2 Fundamentals of friction

One of the most interesting and most important physical phenomenon related to brake systems is the lateral force between two rubbing surfaces, i.e. the friction force. If a block is dragged over a horizontal floor, the lateral force required to move the block is equal to the friction force between the two surfaces.

In the 1490's, Leonardo da Vinci found that when the normal force on the block increases, the friction force also increases [2]. He furthermore discovered that the friction force between to rubbing surfaces is independent of the apparent, nominal, contact area, see Fig. 2.

Two hundred years later Amonton rediscovered what da Vinci already had observed and he formulated "Amontons' laws of friction":

1. The force of friction is directly proportional to the applied load.
2. The force of friction is independent of the apparent area.

These relations between the normal force, F_N, and the lateral force, F_L, can be mathematically formulated as:

$$\mu = \frac{F_L}{F_N} \tag{1}$$

Where μ is the *coefficient of friction*. For many materials this relation is true, within limited load intervals.

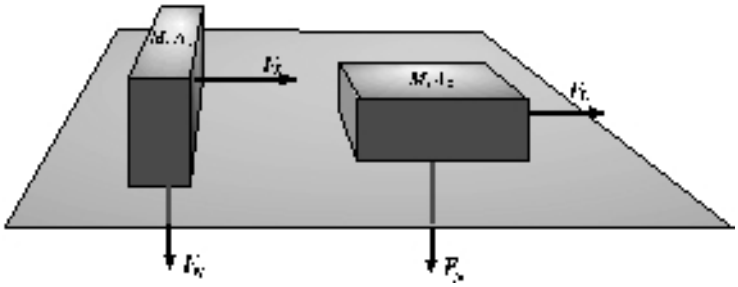

Fig. 2. When a block is dragged over a horizontal surface, the lateral force F_L required is equal to the friction force between the block and the surface. According to Amonton and da Vinci, the lateral force is independent of the nominal contact area.

In order to explain why the friction force is independent of nominal contact area, one must study the two facing surfaces. All technical surfaces have a roughness, even if some appears very smooth. If two rough surfaces are pressed against each other, only small parts of them will actually contact each other. Consequently, the area of real contact will be very small. As a matter of a fact, the normal load and hardness of the two materials will define the area of real contact [3]. An increased hardness or a reduced load will lead to a reduced contact area, see Fig. 3. Thus, for a given material combination, the real contact area depends on the normal load only and has no correlation to the nominal contact area. If the load is doubled, the area of real contact will also be doubled.

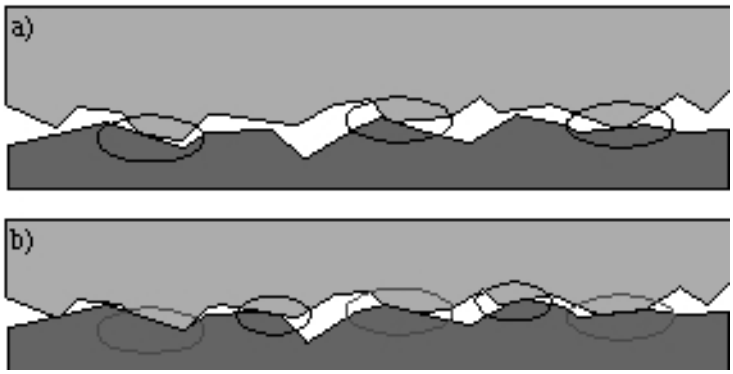

Fig. 3. Contact situation between two rough surfaces. Only small parts of the surfaces are in real contact with each other, encircled. The area of real contact increases with increased load and with decreased hardness.
a) Low load and/or high hardness. b) High load and/or low hardness

In general, the area of real contact is very small. If a 100x100x100 mm steel cube, with a hardness of 3 GPa, rests on a flat steel plate, the nominal contact area is, of course, 10 000 mm^2. The area of real contact, however, is only 0.03 mm^2, a factor 300 000 times smaller [3]!

Now, if the friction force is identified as the force required shearing the real contact between the two surfaces, it can easily be understood that the nominal contact area does not affect the friction force. It can also be understood that a doubled normal load, resulting in a doubled area of real contact, will lead to a doubled friction force.

1.3 Automotive brake systems

An automotive brake system can be divided into three main parts

1. *The rotor*, as the name is indicating, is rotating with the wheel. It is the first part in the *friction couple*. Rotors made of grey cast iron have always dominated the market. The last couple of years, other materials, although still having only a small commercial importance, have been introduced. Some examples are SiC-reinforced aluminium, carbon-SiC composites and sintered carbon.
2. *The brake lining* is the second, stationary, part of the friction couple. During a brake application, the pad is pressed against the rotor with a hydraulic piston. The friction forces between the stationary lining and the rotating disc will turn the kinetic energy of the vehicle into heat.
3. *The hydraulic system* transfers and amplifies the brake force from the brake pedal to the hydraulic piston pressing the linings against the rotor. In modern brakes the hydraulic system also includes the ABS-system (Anti-Blockier System, German) and different kinds of traction systems.

As mentioned in the introduction, a number of different vehicle brake systems has existed over the years. Today two types reign the market, the *disc brake* and the *drum brake*. Drum brakes, being an earlier design, dominated until the 1960´s in all kinds of vehicles. Today, it is predominantly used in trucks and buses. Just recently, disc brakes have been introduced in heavy vehicles as well and will probably have a large share of this market within a few years.

The main difference between the two designs is the geometry of the rotor and linings. The hydraulic systems are similar. Figure 4 shows a schematic picture of a brake system with one drum and one disc brake.

In the disc brake, the linings (also called pads) clamp the disc from opposite sides. The friction force between the pads and the disc are perpendicular to, and does not affect, the normal forces of the pads. Thus, the braking force will depend linearly on the applied normal force, with the premise that the coefficient of friction between the two parts is constant. The result is a superior pedal feel as compared to the drum brake. The lower weight is another benefit with the disc brake.

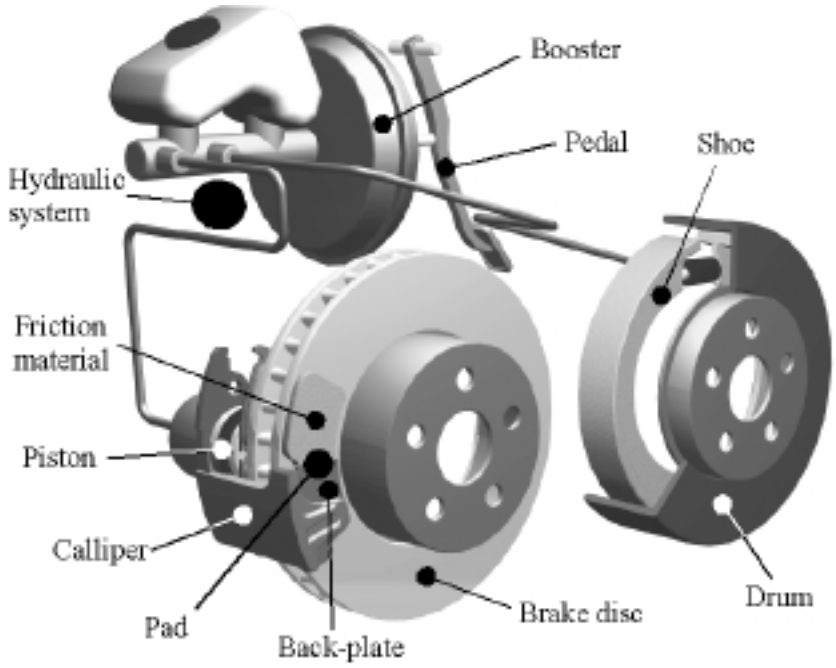

Fig. 4. Illustration of the two brake systems dominating the market, the disc brake and the drum brake. The brake drum and the calliper have been cut open to reveal the pads and shoes. The friction material is cast onto the back-plate, forming the pad. (Karl Åstrand /FZ)

In drum brakes, where the pads (shoes) are pushed outwards against the inside of a drum, the friction force will affect the normal load. Causing the brake to have either a self-locking tendency or the opposite. In either case, the brake system will get a poor linearity and thus a weak pedal feel. The foremost benefit of the drum brake is the insensitivity for harsh environments, such as water, dirt or road salt.

Most heavy vehicles use a pneumatic instead of a hydraulic system to apply the brake force. The brake pedal is connected to a gas valve instead of a piston, controlling the pressure drop from the storage tanks to the brake cylinder. Pneumatic brakes only require a very low pedal force to apply a high braking force, which is needed to stop a truck or a bus. The drawbacks are poor pedal feel and the size of the system. It requires both an air pump and a storage tank.

1.4 Brake pad materials

As mentioned, the first brakes consisted of a rope winded around the back axle of a horse carriage or a piece of wood pressed against the rim of the wheel. When more effective brake materials were needed, an asbestos yarn was spun around the rope, which had been impregnated with tar [4]. Modern lining materials show many similarities with these primitive ropes. Most of them are based on a metal fibre reinforced organic matrix and are called *organic*. There are, however, also other types of lining materials, categorised into *metallic*, *semi-metallic* and *carbon*.

This thesis comprises organic pad materials exclusively. This type will be further discussed below.

Organic pads are generally a compound of a number of different materials. Sometimes up to 20 or 25 different components are used. These components include a:

- *Binder*, that holds the other components together and forms a thermally stable matrix. Thermosetting phenolic resins are commonly used, often with the addition of rubber for improved damping properties.
- *Structural materials*, providing mechanical strength. Usually fibres of metal, carbon, glass, and/or kevlar are used and more rarely different mineral and ceramic fibres. Before its prohibition in the mid 80's, asbestos was the most commonly used structural fibre.
- *Fillers*, mainly to reduce cost but also to improve manufacturability. Different minerals such as mica and vermiculite are often employed. Barium sulphate is another commonly used filler.
- *Frictional additives*, added to ensure stable frictional properties and to control the wear rates of both pad and disc. Solid lubricants such as graphite and various metal sulphides are used to stabilise the coefficient of friction, primarily at elevated temperatures. Abrasive particles, typically alumina and silica, increase both the coefficient of friction and the disc wear. The purpose of the latter is to offer a better defined rubbing surface by removing iron oxides and other undesired surface films from the disc.

In the thesis, a number of different brake pads have been used. One pad, however, frequently recurs in the thesis, the standard pad to the Volvo 850/S70, denoted TX4005. The pad materials are not described in detailed, but more information is found in the appended papers.

1.5 Sound in general and brake squeal in particular.

Vibrating structures cause pressure waves in the surrounding media. These waves are known as sound and the tone we hear depends on the frequency of the vibration, i.e. the number of completed cycles per unit time. High frequencies are heard as high pitch tones and low frequencies as low pitch tones. Frequency is measured in Hertz [Hz], cycles per second. Sound volume, or sound pressure level, is measured in decibel [dB]. The decibel scale is logarithmic and it corresponds well to the hearing impression. A young person with normal hearing can hear sounds from 0 to 130 dB with frequencies between 20 Hz and 20 kHz. A speaking person generates about 45 dB. The pressure level in the close vicinity of a starting jet aeroplane is around 145 dB [5].

The energy transported with sound is generally very small. If a vibrating structure emits sound spherically, i.e. equally in all directions, and causes a sound pressure level of 120 dB on a distance of one meter, the emitted power is only 12 W. At 90 dB, still an annoyingly high sound level, the corresponding power is only 12 mW. It is easy to understand that even a very limited mechanical power being transformed to sound, will generate high sound pressure levels.

The power developed during a stop, estimated in chapter 2, is thus more than a thousand times higher than the largest possible part radiated as sound. Although the power required to overcome the damping of the system is much higher, it is still negligible compared to the energy input from the friction force. Almost all the energy is dissipated in the form of heat.

Brake squeal can be described as an irritating sound with a main frequency between 1 and 20 kHz, generated by the brake components. It is predominantly generated at low speeds (below 30 km/h) and at low brake pressures (brake line pressures below 20 bar). Typical squeal situations are stopping at a red light or in a parking spot.

Furthermore, brake squeal has a stable and dominating main frequency plus a number of overtones, resulting from the different vibration modes of the brake assembly. The modes describe the ways in which the system is allowed to vibrate easily. To achieve other ways of motion than described by the modes, large external forces are required. Frequencies corresponding to the modes are called *resonance frequencies* and the phenomenon when a structure is easily vibrating is called *resonance*. Theoretically, at resonance the amplitude (the magnitude of the movement) is only dependent on the damping of the system and the input energy. Equilibrium is reached when the input energy equals the energy absorbed by the damping. This equilibrium state is referred to as the limit cycle.

The similarities between brakes and stringed instruments are striking, disregarding brake squeal being unwanted and out of tune. The geometry of the brake assembly, or

the instrument, controls the frequency of the emitted sound and the friction between the rubbing parts supplies the energy needed to maintain a sound. There are thus two ways to prevent the sound. One is to modify or damp the resonant system, the violin string and box or the disc and pads. You can fill the violin box with some soft stuffing and you can glue damping rubber shims on the back plate of the brake pads. The second way to prevent sound is to change the friction mechanism so that the necessary conditions for sound generation are never accomplished. On the violin it is relatively simple, you just do not put resin on the bow. In a brake it is, however, more difficult. A reduced friction will impair braking performance and stopping the car will become more difficult. However, squeal generation is influenced by many other friction characteristics in addition to the friction level, so it might be possible to design a brake with a high coefficient of friction and still a low tendency to squeal.

Warranty costs correlated to brake squeal has been estimated to 100 million ECU annually, in Europe alone [6]. Nevertheless, squealing brakes are not only a matter of money. They are also an issue for the acoustic environment in cities. Anyone, who has been waiting for the bus on Drottninggatan in Uppsala, knows what a squealing bus brake echoing between the house walls can do to a persons hearing.

1.6 Squeal testing

Regular brake testing is performed by brake dynamometer testing or by vehicle testing. A brake dynamometer is basically a huge flywheel connected to the brake rotor via an axle. The flywheel is dimensioned to give a kinetic energy corresponding to the vehicle of interest. Each time a stop is to be simulated, an electric motor accelerates the flywheel to the desired speed. During the following brake application, the wheel is disconnected from the motor and decelerated with the brake.

In the present work, a slightly different laboratory technique, based on a real automotive disc brake, has been used. An electric motor, directly connected to the brake disc via a gearbox, controls the deceleration independently of the brake force. This technique is more flexible for squeal testing, but is restricted to low speed testing only.

The test equipment was chosen as a compromise between the flexibility of a simplified laboratory test and the relevance of vehicle testing. A pin-on-disc machine or a miniature brake assembly may give equally relevant friction results and perhaps more conveniently provide samples for surface analysis. Although often possible, scaling temperature, speed and brake pressure between a real and a laboratory set-up is difficult. Furthermore, when studying brake squeal, the geometry and detailed design of the system is of vital importance. A miniature brake would never give the same resonance frequencies as a real assembly. Due to the resulting squeal frequencies being related to the test conditions, a mini-brake would never give satisfactory results. The present test equipment, however, gives the opportunity to produce relevant squeal testing in a manageable and flexible set-up.

Test equipment

All brake tests in the thesis were performed in the same test equipment. This rig is based on a front wheel suspension from a Volvo 850. It is a complete front left corner including spring strut and lower wishbone, Fig. 5. The wheel is driven by an electric motor via a gearbox and the original drive shaft and rotational speeds can be adjusted between 0 and 4 rps. Brake line pressure is supplied and controlled by a hydraulic system with a servo-valve and can be adjusted between 0 and 30 bar. A schematic picture and a photograph are shown in Fig. 5

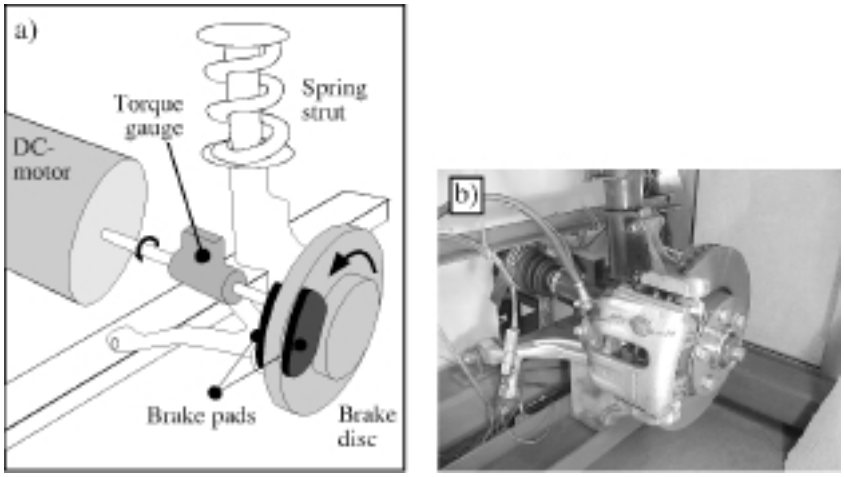

Fig. 5. Test rig for squeal testing. During testing a wheel is mounted on the hub. a) Schematic and, b) Photo of the test rig.

During the squeal tests, the brake-line pressure, brake torque, disc temperature, sound and relative air humidity are registered, typically every third second.

The braking torque is measured with a torque gauge mounted on the drive shaft. Given the radius of the disc, the coefficient of friction can be calculated. Some difficulties do, however, occur as the calliper clamps around the disc. The clamping force deforms the calliper and, as a result, the centre of the clamping force is shifted away from the centre of the disc. The effective radius of friction is increasing, meaning that the friction measured via the torque is an over-estimate of the real friction force. When searching for brake squeal, comparatively low clamping forces are used and the deformation will only have limited effect on the measured coefficient of friction.

A microphone inside the covering chamber picks up the emitted sound. After amplification, a snapshot of the signal is sampled into a digital oscilloscope. This snapshot is now transferred to the measurement computer via GPIB. In the computer it is further band-pass filtered and if the sound pressure level exceeds 78 dB the sound is classified as a squeal, analysed using fast fourier transformation (FFT) and saved to

disc. As an extra analysis after the test, the FFT-spectrum is used to sort out unwanted sounds, i.e. sounds with a main frequency below 1 kHz.

If the number of sounds classified as squeals is divided by the total number of measurements, the squeal index (S.I.) is obtained. Figure 6 illustrates sound, pressure and speed measurements during one stop. In the illustrated case the squeal index is 2/7≈0.29. The squeal index is thus a measure of the probability for a brake squeal to be generated during the given conditions.

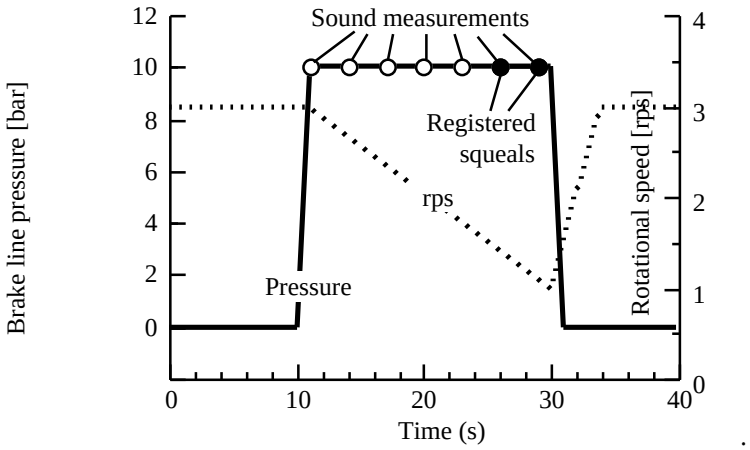

Fig. 6. Schematic of sound, pressure and speed during one stop. If the number of registered squeals, filled circles, is divided by the total number of sound measurements, circles, for one stop, the squeal index for that stop is obtained. In the illustrated case the squeal index is 2/7=0.29.

Test procedure

Almost all squeal tests were performed using test programs based on 42 stop sequences. The sequences may look a little peculiar but have been designed to cover a wide as possible range of temperatures and pressures. The sequence has been redesigned a few times in order to cover an even wider range of temperatures and pressures. The two most frequently used sequences are shown in Fig. 7. Sequence II not only covers a wider range of pressures, but thanks to the higher brake pressures, it also spans over a larger temperature range than do sequence I.

Longer periods between the stops have sometimes been used in order to lower the test temperatures without modifying the pressure sequence. Generally, the idle periods were set to 100 s.

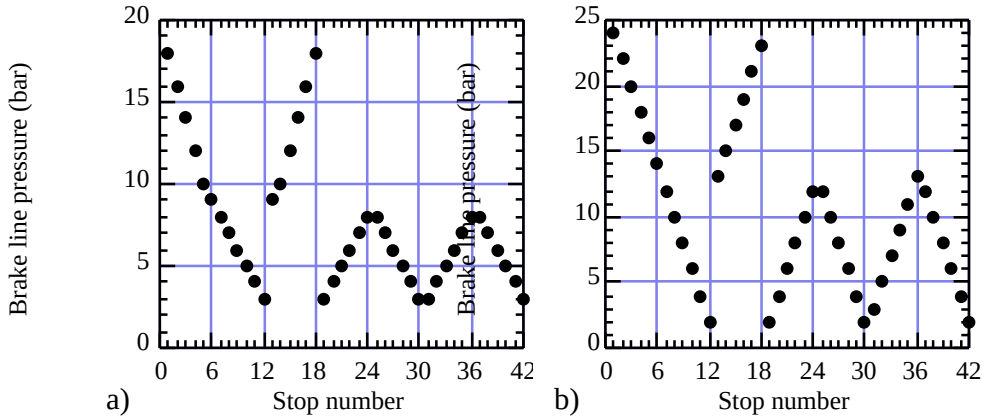

Fig. 7. Pressure cycles for the two main squeal test programs used in the thesis. Note the different y-axis scales.
a) Sequence I, with a maximum line pressure of 18 bar.
b) Sequence II, with a maximum line pressure of 24 bar.

Either of sequences I or II is normally repeated 5 times to form a complete test. The test thus includes 210 stops. During each stop (also referred to as braking), the rotational speed is reduced from 3 to 1 rps in 20 or 30 s. With a sampling rate of 1/3 Hz the total number of measurements during one test has varied from 1400 to 1900. Note that a sound snapshot, with a sampling frequency of 100 kHz, also is taken at the same rate as the analogue signals.

Some investigations required a higher sampling rate than generally used, for example to study the friction and sound variations over each revolution of the rotor in Paper III. In these cases an analogue band-pass and rms.-filter was used to get a scalar value of the sound intensity at any given time. This value could be measured at a high frequency, together with the other analogue signals.

All pads have been tested without damping shims or any other squeal inhibiting mechanical additives.

2 TRIBOLOGICAL CONTACT IN BRAKES

Automotive brakes constitute one of the few applications where a material is supposed to slide against another, at high sliding velocities with a high coefficient of friction. This puts extreme demands on the friction materials. They need a stable friction at different temperatures, loads, environments and stages of wear. Furthermore, seizure, excessive wear rates and macroscopic fracture must be avoided.

An illustration of the power development in a car brake is given by the following example. A modern midsize car weighs about 1500 kg. When driving at 28 m/s (~100 km/h), the kinetic energy of the vehicle is 600 kJ. The shortest possible distance within which the car can be stopped is about 40 m. Assuming that the retardation is constant, which is reasonable since the friction between tyre and road controls the retardation force, this will take 2.9 s. As a result, the average power developed will be 206 kW and the maximum power, in the beginning of the stop, will be 412 kW. Approximately 80 % of this power is absorbed in the front brakes and these have two brake pads each. The maximum power absorbed in each pad is thus 82 kW, a value similar to the maximum engine output. All this power is developed in an area slightly smaller than the size of a hand. The area of real contact, however, is even smaller. Although very difficult to calculate, we can conservatively estimate it to 20 % of the nominal area. This will be further discussed in the next section. Now imagine that the deformed layer between the pad and disc is 1 μm thick, which also will be shown being a reasonable estimate. The total deformed volume is thus 0.8 mm^3 = $0.8*10^{-6}$ dm^3 (litres). The power developed in the deformed layer is thus 100 GW/dm^3. As a comparison it can be mentioned that a nuclear power reactor develops around 1 GW.

2.1 Microscopic contact situation

The contact situation in the pad/disc friction couple is largely undocumented in the literature. Generally, the disc surface has been found to be shiny, rather flat and free from thick tribofilms [7]. A major part of the present thesis has been focused on exploring this contact, using a number of modern techniques, including SEM, optical profilometry and nanoindentation in Paper VIII, light optical microscopy (LOM) and macro photography in Paper V and video recorded high magnification in-situ studies of pad material against a glass disc in Paper VII.

Normally, brake pads are composites of materials with very different properties. The weakest components, such as resins and solid lubricants, have a hardness of around 200 MPa, while the abrasive particles and fibres in some cases may have a hardness of up to 20 GPa. The components show a correspondingly wide spectrum of wear resistances. These differences result in a complex contact situation. Unevenly distributed wear and compaction of wear debris results in a surface characterised by flat plateaus, rising above the rest of the surface.

The plateaus can be spotted with the naked eye as shiny spots scattered over the pad surface. A scanning electron microscope (SEM) or a profilometer reveals that the

plateaus are of varying sizes, typically between 50 and 500 µm in diameter and a few microns high. They can be defined as the areas of the pad showing signs of sliding contact with the disc. Typically, these signs involve a relatively flat surface with shallow grooves in the sliding direction, see Fig. 8. The number of plateaus on one pad is typically on the order of 10^5 and their total area is 10-30% of the nominal area of the pad.

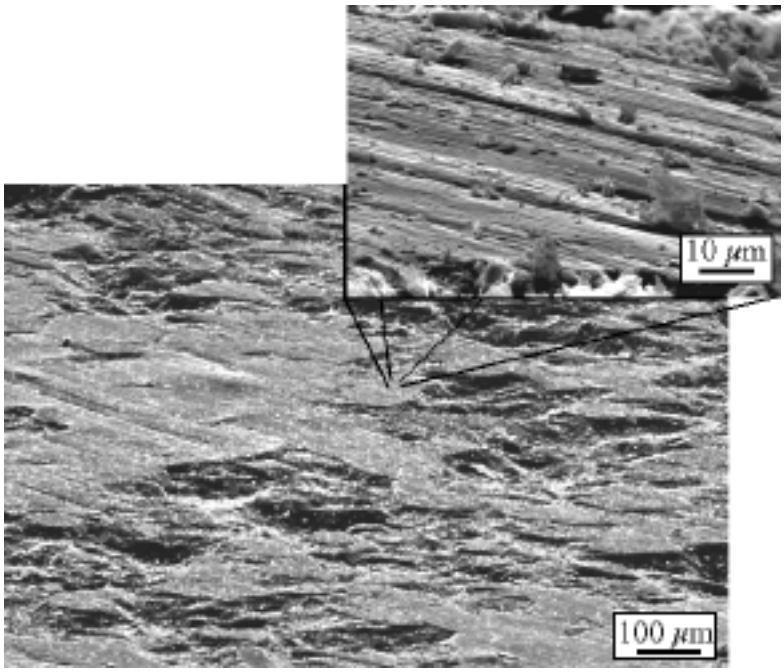

Fig. 8. Contact plateaus forming the surface landscape on an organic brake pad. The grooved surface typical of contact plateaus is visible in the inset picture. (SEM)

To facilitate an effective description of the contact situation, two new expressions have been coined: *primary* and *secondary plateaus*. These are defined and further discussed in the following sections. The primary and secondary plateaus together form the contact plateaus.

As in all other sliding contact situations, the area of real contact transfers the friction forces. Due to the topography of the brake pads, the area of real contact is confined within the contact plateaus, Fig. 9. The size and composition of the plateaus thus has a crucial influence on the friction behaviour of the pad.

The presented contact situation is unique for the given material combination, with a coarse inhomogeneous composite sliding against a solid metal disc. If the brake pad is replaced by a piece of solid cast iron with the same geometry, a completely different situation would occur. The number of contact areas would be much fewer, due to the

higher stiffness of the iron. Lining materials are generally more compliant than solid metals and thus, the contact areas will be more evenly scattered over the surface. If a plateau experiences a high load, the low modulus of the matrix will help to unload it. The load will be transferred to the neighbouring plateaus, resulting in a more evenly distributed load.

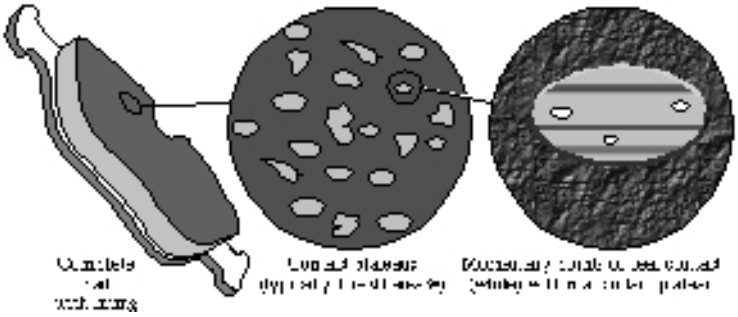

Fig. 9. General view of the brake pad area and its division into contact plateaus and areas of real contact within the contact plateaus.

Surface roughness of disc and pad

The tribological conditions of the pad material result in a rough surface, with a typical R_a of 2 µm, see Fig. 10. In the profile, two contact plateaus can be spotted as 0.1 mm wide and relatively flat areas. Generally, the surfaces of two well run-in mating parts in sliding contact exhibit matching profiles. This is not valid for the brake pad and disc couple, as evident from comparing their profiles perpendicular to the sliding direction in Fig. 10. The profiles of the plateaus, however, match those of the disc, see Fig. 10b.

Furthermore, the uniform sliding of the plateaus against the disc results in a surface with different roughness in different directions. Parallel to the sliding direction, the two surfaces in contact are very smooth, while perpendicularly they are more than twice as rough. The plateau is slightly rougher than the disc in both directions. The grooved appearance of the disc surface is visualised by the surface plot in Fig. 11.

Formation of contact plateaus

Contact plateaus consist of two parts, *primary plateaus* and *secondary plateaus*. The primary plateaus first form due to the lower removal rate of the mechanically stable and wear resistant ingredients of the pad. In a second stage, these protruding hard phases may form nucleation sites for the growth of secondary plateaus. In Paper VII, it was observed that debris, in the form of small particles, constantly flows through the maze of shallow channels, formed between the pad and disc. Occasionally, the debris becomes jammed and piles up against the primary plateaus, or secondary plateaus if such already exists, blocking their way, see Fig. 12. The normal pressure, shear forces and the friction heat combines to compact the debris and the secondary plateaus grow.

Figure 13 shows the topography and the composition of two contact plateaus, including both secondary and primary parts (Paper VIII).

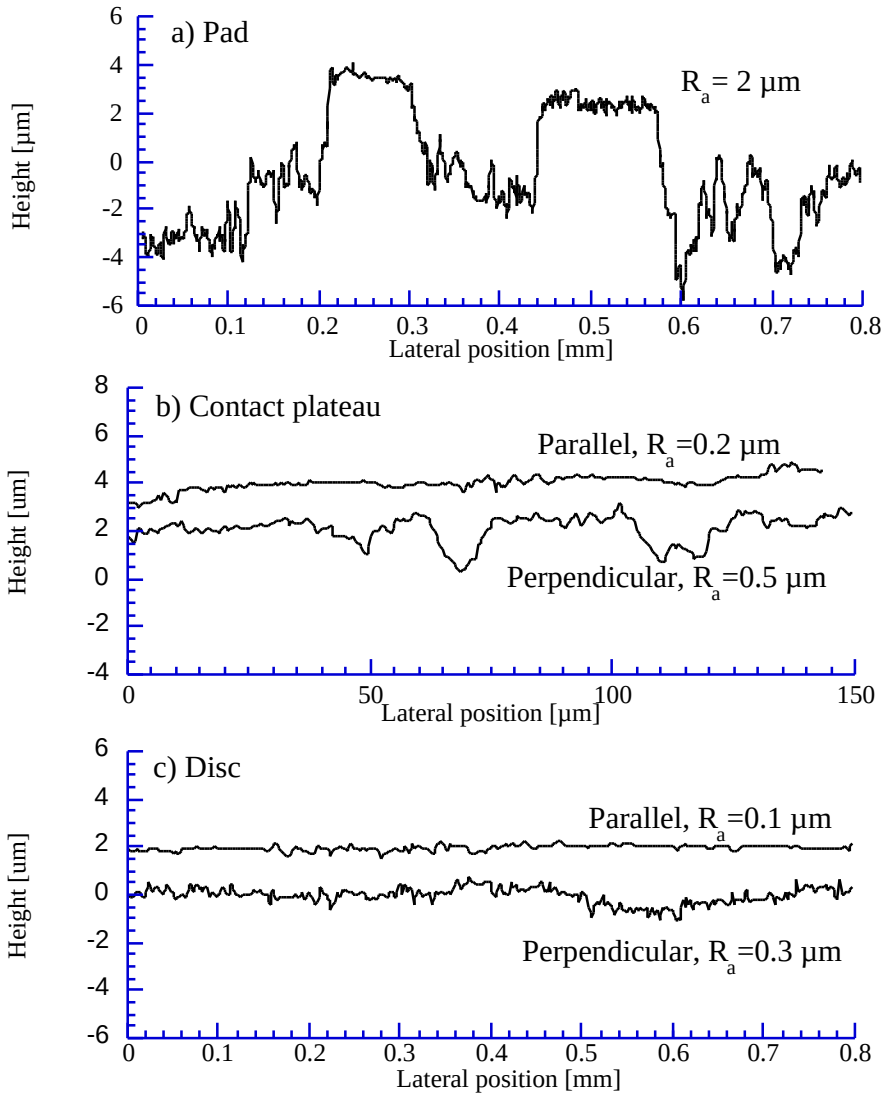

Fig. 10 Surface profiles of the friction couple. (optical profilometry)
a) pad, including two contact plateaus,
b) contact plateau measured parallel and perpendicular to the sliding direction,
c) disc measured parallel and perpendicular to the sliding direction.

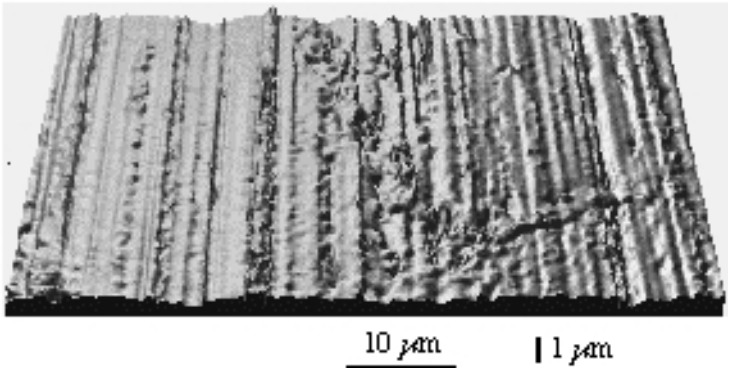

Fig. 11. Topography of a brake disc surface. Sliding direction of the pad: inwards. (optical profilometer)

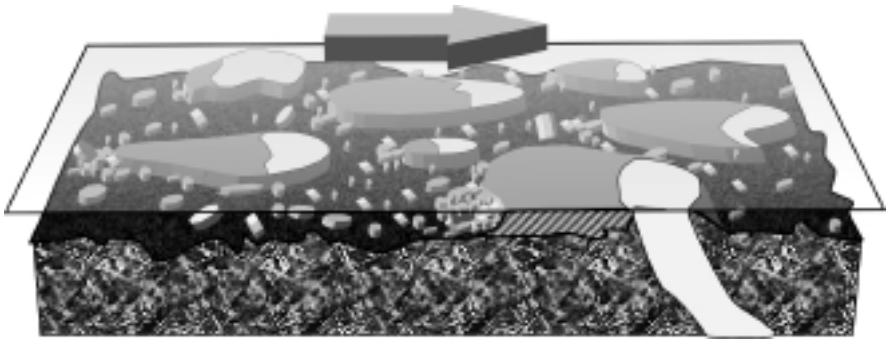

Fig. 12. Schematic of the contact situation between an organic brake pad and a brake disc, involving contact plateaus with primary (lighter) and secondary parts, and a flow of debris, partly piling up against the plateaus. A steel fibre constituting a stable primary plateau and a secondary plateau formed in front of a fibre, are visible in the cross-section. The frictional energy helps to compact and sinter the debris forming the secondary plateaus.

The build-up of compacted areas requires supply of wear debris, a limited space between pad and disc, friction energy and normal load. Thus, the formation of the secondary plateaus is a gradual process. Nevertheless, during favourable conditions it can form in less than a second (Paper VII). The propensity to form plateaus, affects the in-stop friction increase. In Paper V, it was observed that more wear debris was gathered on the pad surface in dry air than in humid. It could not be confirmed by microscopy that larger plateaus form at low humidity, but the friction behaviour gave such indications. When braking in dry air, the average friction and the in-stop friction increase was high.

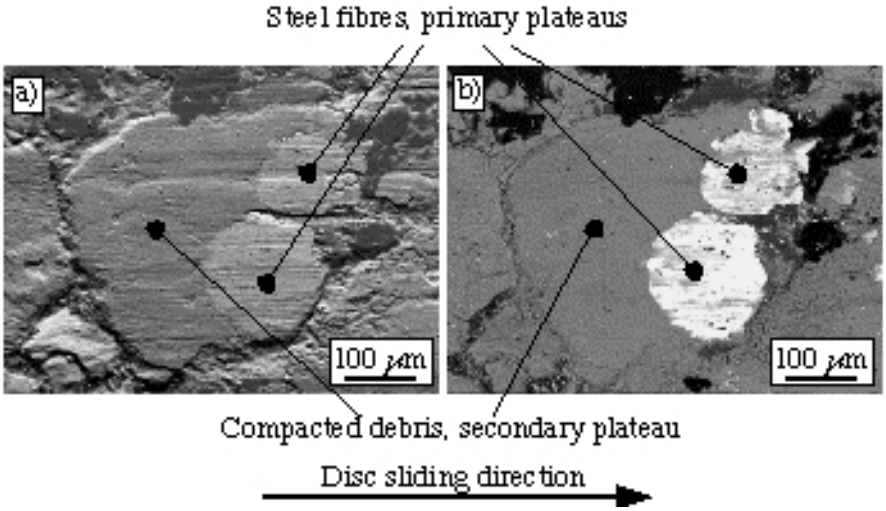

Fig. 13. One of the 10^5 contact plateaus seen on the surface of an organic brake pad. Note the two primary plateaus, steel fibres, supporting the secondary plateau, compacted debris to their left. (SEM)
a) Enhanced topographical contrast. b) Enhanced compositional contrast.

The lowlands surrounding the plateaus consist of less wear resistant pad constituents, such as polymeric resins, fillers, and friction modifiers. These are mechanically weak and worn mainly through three-body abrasion (Paper VII). Wear debris generated in the contact is tumbling in the labyrinth between disc and pad, milling down the weaker constituents forming the lowlands. During the process, the debris is reduced in size by fragmentation and wear. When the particles are small enough, they will either take part in the formation of contact plateaus or leave the contact.

The secondary plateaus cannot exist without the support from the structural components of the pad, the primary plateaus. In Paper VII, it was shown that the secondary plateaus will degrade within parts of a second after loosing their support. The loss may be due to wear or detachment of the fibre. Dirt or irregularities in the disc surface can also degrade the plateaus. This degradation is instantaneous, a secondary plateau is ruined immediately, when hit by a surface defect on the passing disc.

Analogous to the surrounding lowlands, the secondary plateaus are worn through three-body abrasion and erosion by wear debris transported through the contact. They are also worn by direct contact with the disc surface. When these wear mechanisms dominates over the formation mechanisms, the secondary plateau will degrade, even with the support from a primary plateau.

The secondary plateaus further require relatively stable conditions and a sufficient normal force to exist. Each time the brake pressure is reduced during sliding, large parts of the compacted areas will peel off in flakes, Paper VII. This will naturally affect the appearance of the fully unloaded surfaces we can observe in the microscope, after the actual brake application.

Plateau size

The size of the contact plateaus was investigated in Papers I, IV and VII. It was shown that the size of the plateaus varied with the brake pressure. During mild brake applications, the average size of the plateaus is 50 to 500 µm and they constitute 10-30 % of the nominal pad area, see Fig. 14a. In some cases, involving high temperatures and brake pressures, the plateaus can grow to over millimetre sizes and may cover the main part of the pad, see Fig. 14b.

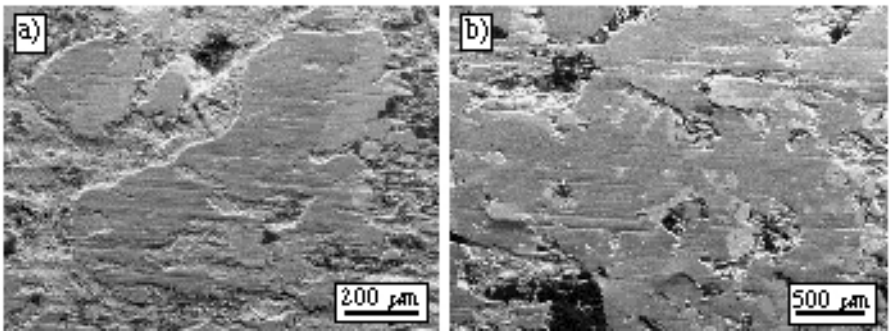

Fig. 14. Contact plateaus on standard pad to a Volvo 850 after braking at a) low brake pressure and temperature and b) high pressure and temperature. Note the different scales. Disc sliding direction: left to right. (SEM)

This growth phenomenon may be due to two mechanisms. The primary explanation is that the increased load will reduce the space between the pad and disc. When the height of the narrow passages in this labyrinth is reduced, more debris will become jammed and thus the secondary plateaus grow, as apparent from Fig. 12.

The second reasonable explanation is the effect of the increased temperature and the increased pressure itself. Wear debris will be more prone to sinter, forming agglomerates or even continuous films, at high loads and temperatures than at low.

However, the growth can not be explained by the need for a larger contact area to carry the higher normal load, as the existing primary plateau area is already over-dimensioned. A process based on the need for a larger load carrying area would have to operate much faster than the observed changes. It would require an almost instantaneous response to the load increase.

When the load is decreased, the deterioration mechanisms will dominate over the formation mechanisms and the size of the secondary plateaus will be reduced.

Microstructure and mechanical properties of secondary plateaus

The microstructure of the secondary plateaus varies with the depth from the surface. Close to the surface, the material is dense and extremely fine-grained. A continuous tribofilm with grain sizes in the nanometer range is formed, see Fig. 15. Figure 16

shows the surface of a secondary plateau in high magnification. A diffuse structure can be spotted in, or just below the surface, with 5-10 nm grains. On top of the nano-particle layer, an extremely thin and fine-grained, or amorphous, layer is believed to be found. This layer is only a few nanometers thick and can therefore only be discerned as a blur, covering the grains in Fig. 16. This ultra-thin top layer will not be discussed further.

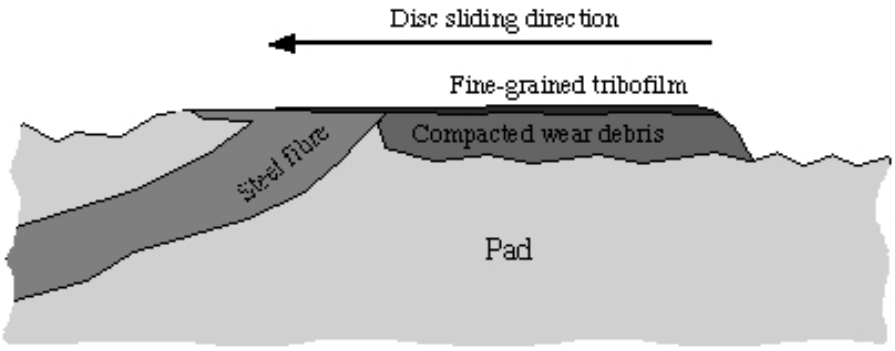

Fig. 15. Schematic cross-section of the wear debris, fine-grained tribofilm and fibre forming a contact plateau.

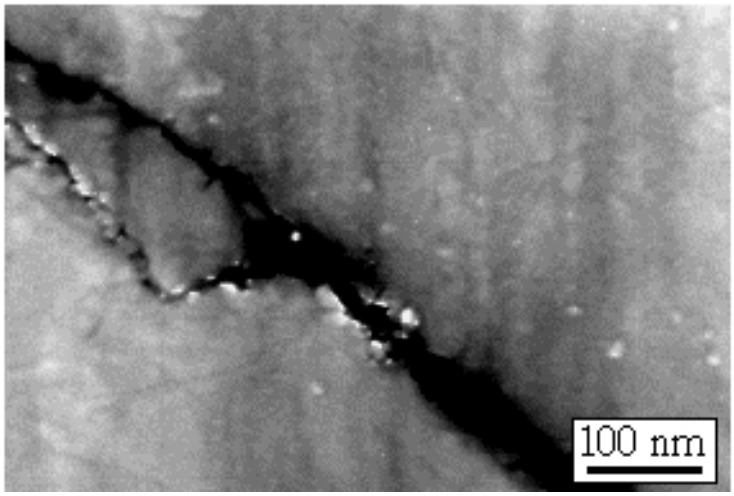

Fig. 16. Surface of a secondary plateau on an organic brake pad as formed by the contact against the disc. The agglomerated particles forming the tribofilm covering the plateau surface are smaller than 10 nm. (SEM)

The backside of a detached piece of a secondary plateau can be seen in Fig. 17. It is characterised by loosely compacted particles that are considerably larger than the particles seen in the front surface. A typical size range is 0.1 to 1 µm, where the bigger particles appear to be agglomerates of smaller particles, less than 0.2 µm.

The fine-grained top-layer is less than 1 µm thick. Below this layer, the particle size is fairly independent of depth, see Fig. 18. High pressure, shear force and surface temperature is believed to be responsible for the homogenisation, sintering, of the top–layer.

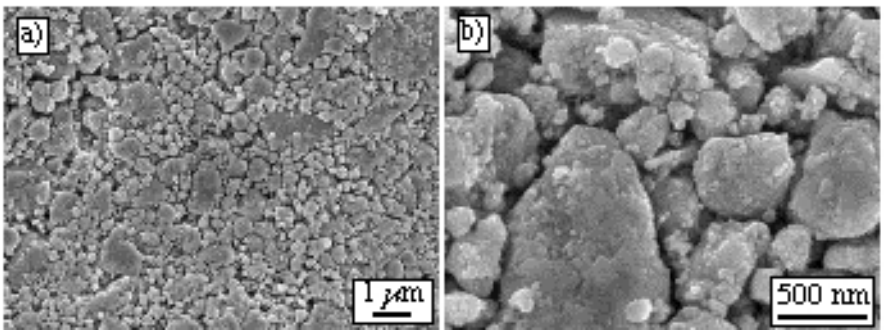

Fig. 17. Backside of a detached fragment of a secondary plateau studied in two magnifications. This surface was facing down towards the matrix material. The grain size is much larger than in the tribofilm on the surface in Fig. 16. (SEM)

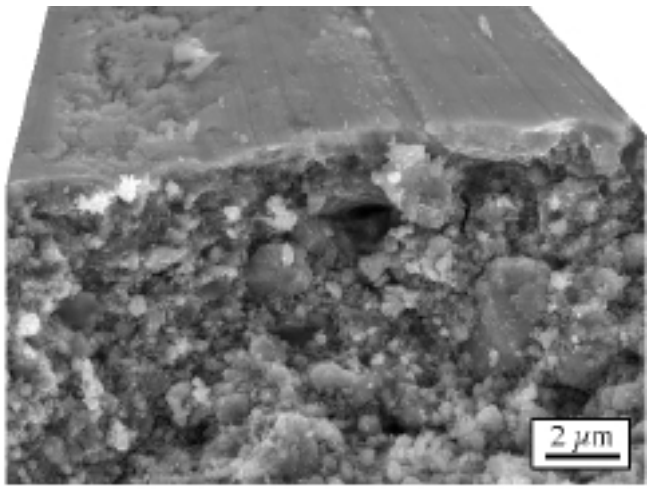

Fig 18. Fracture cross-section of a secondary plateau. Note the thin homogeneous top layer and the transition to a coarser structure below. Sliding direction of the disc: inwards. (SEM)

The secondary plateaus have a relatively high compressive strength but poor tensile strength (Paper VIII). They are only loosely attached to the primary plateaus and the underlying matrix material. This is due to their formation from a pile of jammed debris. The top layer is "ironed" and effectively compacted by the sliding contact against the disc surface, while the interior is only marginally compacted and heated.

Nanoindentation of a secondary plateau indicated hardness values between 0.2 and 3.9 GPa, depending on the depth of indentation. When indenting only 50 nm, the hardness value is considerably higher than for 400 nm and 1 µm indentations. This indicates that the fine-grained surface layer is much harder than the underlying layer of compacted debris. These values can be compared to the hardness of the steel fibres, 3.7 GPa, see Fig. 19.

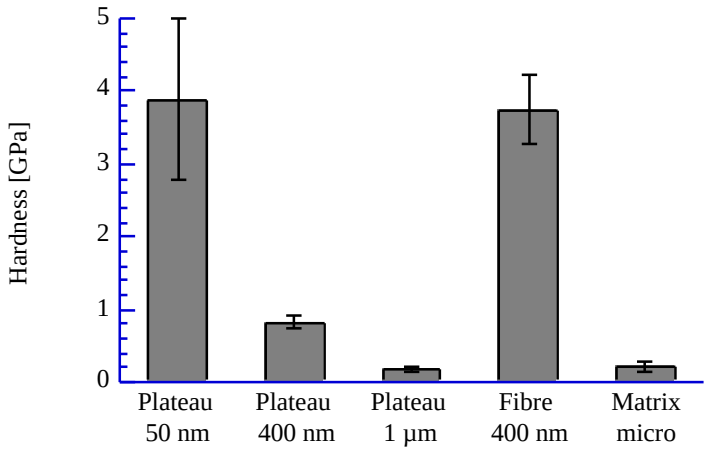

Fig. 19. Nanoindentation hardness values for the secondary plateaus at 50 nm, 400 nm and 1 µm indentation depth. The values are compared to the hardness of a primary plateau, steel fibre, at 400 nm indentation depth and the matrix hardness as measured by microhardness testing.

The plateau hardness as measured with 1 µm indents is comparable to the 0.2 GPa hardness of the underlying matrix, as measured using regular microhardness indentation. This is not surprising, since the thickness of the top-layer of the secondary plateau is less than 1 µm and the depth of the elastic deformation can be estimated to 10 times the indentation depth, which exceeds the total thickness of the secondary plateau.

If a secondary plateau is scratched with a scalpel, it will crack and loose adhesion to the underlying matrix material, see Fig. 20. The flakes formed, revealing a typical of 5–10 µm thickness of the secondary plateaus, show no signs of plastic deformation. This relatively brittle behaviour is not surprising, considering their porous micro-structure. The fine-grained top layer, showing high hardness and a dense microstructure, probably acts as a protective coating when the plateaus are tribologically loaded.

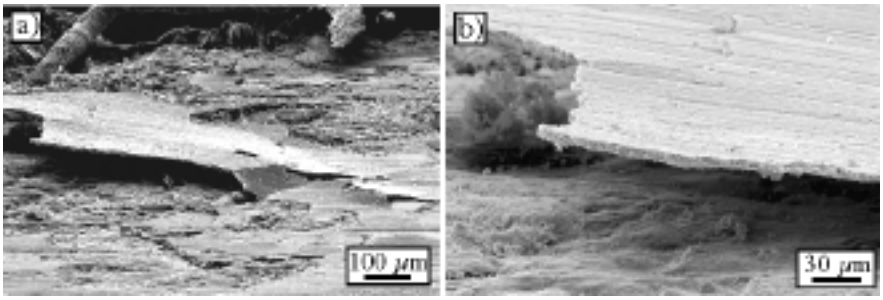

Fig. 20. A flake of a secondary plateau has been detached from the pad with a scalpel. Some parts of the plateau still adhere to the surface. (SEM)

Composition of the plateaus

The composition of the contact plateaus is dominated by iron, in the form of iron oxide in the secondary plateaus and in the form of steel in the primary plateaus. Quantitative EDX-analysis have shown that the ratio between iron and oxygen within the secondary plateaus is 4/5, see Table 3. Furthermore, the debris is almost exclusively black, see Paper V. This indicates that FeO and/or Fe_3O_4 dominate the plateaus.

Jacko et al. have shown that wear debris is more easily compacted when containing more organic components [8]. However, the secondary plateaus studied in this thesis showed no signs of carbon.

Table 3. Composition of a secondary plateau on the standard pad to Volvo 850. (EDX-analysis in the SEM)

Element	Weight-%	Atomic-%
Iron	65	40
Oxygen	25	52
Copper	5	3
Silicon	3	3
Sulphur	2	2

2.2 The influence from plateau growth and degradation on the coefficient of friction

When the secondary plateaus grow, e.g. due to a load increase, the primary plateaus will keep their size and thus the average composition of the material sliding against the disc changes. The grown compacted areas consequently will carry a larger share of the normal force and thus the friction conditions are different.

As the composition of the plateaus changes with changed load, the friction force needed to shear the top-layer can be expected to change. Further, if the plateaus are adapted to a

certain brake pressure and the pressure is decreased, the coefficient of friction should be expected to change. The macroscopic effects of these processes can be observed for some brake pads as a friction hysteresis, discussed below.

During the initial run-in of a green (unused) pad, a large increase in friction can be observed during the first stops. This behaviour is due to the formation of primary plateaus. The phenomenon is further discussed in chapter 3.

In Paper II, it was observed that defects, in the form of pits in the disc surface considerably lowered the coefficient of friction. The decrease is believed to be a result of a continuous degradation of the contact plateaus. Each time a plateau is hit by a surface defect, the secondary plateau will be degraded, and thus the coefficient of friction will be lowered.

3 DYNAMIC BEHAVIOUR OF THE CONTACT SURFACES

As discussed in Paper IV, the size of the area of real contact between the pad and the disc, and also the composition of the outermost surface layers within this area, is far from constant but will vary due to changing pressure, changing temperatures, deformation and wear. The contact pressure may vary on different time scales and both locally and globally, due to different processes.

3.1 Rapid processes

Rapid global processes

Naturally, a change in the braking force will result in a corresponding change of the elastic compression of the pad. The actuation and variation of the braking force can be quick due to manual “fine tuning” during a braking or due to ABS brake power variations, etc. The associated pressure changes are global over the brake pad (the average compression of the pad varies) and on a time scale of 1/10 s. Ideally the resulting braking power should be proportional to the pedal force.

A quick brake pressure increase thus momentarily results in a corresponding elastic compression of the pad. This compression will result in:

- more contact plateaus becoming engaged, as shown in Fig. 21a.
- a redistribution of the load between primary and secondary plateaus within each contact plateau. When the load is increased on one plateau, the mechanically more stable part will carry a larger share of the load. Thus, the average composition of the material transferring the load to the disc will change.
- an increased load on the already engaged contact plateaus, which will result in a higher area fraction of real contact within these plateaus, see Fig. 21b.

Rapid local processes

The pad compression, and hence the pressure, may also vary locally over the pad surface. Vibrations cause rapid local pressure variations in the brake system, such as brake squeal, see e.g. [9-11]. Brake squeal vibrations are associated with bending and wave motions of the pad and disc. These deformations result in local pressure variations over the contact surfaces, often on a time scale of milliseconds or less.

The mechanisms for contact area variations are the same as in the global processes.

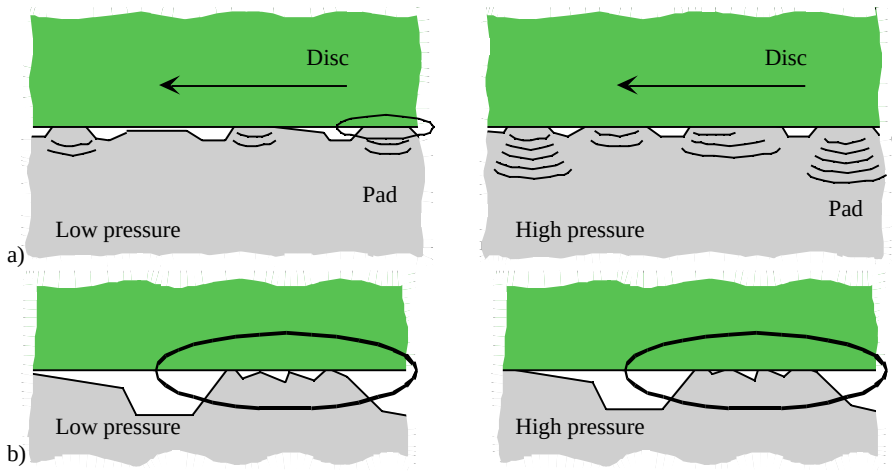

Fig. 21. Illustration of the mechanisms for rapid contact area variation.
a) The elastic loading and unloading of contact plateaus, i.e. the number of engaged contact plateaus increases due to the elastic deformation of the pad.
b) The area fraction of real contact within individual plateaus increases due to local plastic deformation.

3.2 Slow processes

In addition to the rapid mechanisms of contact area variation, a number of slow mechanisms are operating. These become important in determining the nature and size of the contact area if sufficient time (or sliding distance) is allowed. The slow processes are due to different kinds of wear and accumulation of debris, and to temperature variations. They typically appear on time scales of seconds or more, such as during long, low decelerating brakings or as the accumulated result of numerous brakings.

Slow processes appear both on a micro-scale, that is on the scale of individual contact plateaus or smaller, and on a macro-scale, that is on a scale involving numerous plateaus.

The slow processes, which will be discussed below, include:

- Formation, growth and disintegration of contact plateaus
- Shape adaptation on a micro level
- Shape adaptation on a macro level
- Thermally induced deformation on a macro level
- Thermally induced surface property variations
- "Contamination and cleaning" processes

Formation, growth and disintegration of contact plateaus

The growth and disintegration of contact plateaus involve agglomeration and compaction of pad wear debris around a wear resistant nucleus, as discussed in a previous section.

Shape adaptation on a micro level

When the load on a contact plateau is increased, the small areas of real contact within the plateau will flatten elastically, plastically and by wear. These processes result in an increased area of real contact against the disc.

When the load is decreased, the wear and deformation of the points in real contact will tend to reduce their contact with the disc.

Shape adaptation on a macro level

The disc is continually worn, chiefly by the harder components in the pads. This wear will initially polish the disc surface, making it better adapted to the pad. The individual contact plateaus on the pad will correspondingly experience milder contact conditions along the less rough sliding path.

Due to the inhomogeneous structure of the materials, the continuous wear on both the disc and the pad will not be evenly distributed. However, the mutual adaptation to the shape of the counter surface will result in a wavy surface. On the disc, the waves will form concentrical circles. In an ideal steady state situation, the matching between the two parts is perfect, and each individual contact plateau will experience a smooth ride. However, small misalignments or movements between brakings or due to other changes, will result in mismatched surfaces and initially a reduced area of real contact.

Thermally induced deformation on a macro level

During moments of high and increasing temperature, the pad surface will be hotter than the interior and the back plate. This will result in convex bending of the pad and hence an uneven pressure distribution, see Fig. 22. The pressure reduction on the leading and trailing edges will result in a corresponding uneven distribution of wear; i.e. the pad will become thinner in the centre.

When returning to a lower temperature, the pad will straighten out. Now, the uneven wear during the bent situation will result in reversal of the uneven pressure distribution.

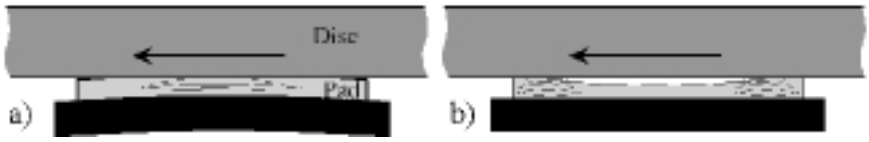

Fig. 22. Mechanism for uneven pressure distribution and uneven wear due to thermally induced distortion of the pad and plate. a) A hot surface will give the pad a convex bend. b) When returning to lower temperatures the pad will straighten, but wear during the bent situation has now resulted in an uneven shape and a corresponding uneven pressure distribution.

Thermally induced surface property variations

The properties of any surface depend on the prevailing temperature. When the disc and pad are heated during braking, this will affect both the chemical reactivity on their surfaces, the mechanical properties (thermal softening, etc.), the structure of the pad (decomposition of polymer constituents, etc.), the tendencies for smearing and sticking of wear debris on both surfaces, etc. Both the composition and the tribological properties of the surfaces are affected.

”Contamination and cleaning ” processes.

Unloaded contact plateaus are exposed to different “contamination” processes, including oxidation, smearing out of wear debris and road dust, etc., which will change their composition. When the sliding contact is continued the plateaus will be subjected to a “cleaning” process involving the removal of the less wear resistant surface layers. This cleaning results in an increased degree of metallic contact. The corresponding processes occur on the disc surface.

The slow contact surface variation processes are responsible for:

- the in-stop increase of μ during long brakings,
- the μ hysteresis reported for brakings under varying pressures,
- the μ increase during running-in of a new disc or a new pad,

all of which effects will be further treated in the following section.

4 FRICTION AND SQUEAL IN BRAKES

4.1 Variations in the coefficient of friction

All mechanisms described in 3.2 correspond to variations in the coefficient of friction. Friction variations due to rapid processes are difficult to measure. The wheel inertia constitutes an effective low-pass filter, removing all high frequency components in the torque signal. A close to the surface friction gauge is necessary to measure the rapid variations. Slow processes, on the other hand, are more easily observed. They include the in-stop friction increase, the friction hysteresis and increase during run-in of a new pad or disc, mentioned above.

Friction increase during run-in of a new disc or pad

When applying a brake for the first time with a new pad or disc, the rubbing surfaces are rough. The as-manufactured disc has a spiral ridge pattern resulting from the turning operation and the as-manufactured pad surfaces have not developed its typical surface structure. During the initial stops, the ridge is gradually worn down and the structural components of the pads are worn flat, forming primary plateaus. The resulting friction increase during this run-in process is generally much quicker for the pads than for the disc, see Fig. 23. Only 5 stops are required for the pad to reach some stable friction level, while the lower friction due to an incompletely run-in disc lasts for 30 stops. In this case the green surface of the pad, was achieved by grinding with a 60 mesh SiC–paper.

In-stop friction increase

During each stop in Fig. 23a, a substantial friction increase can be observed. This phenomenon has been denoted *the in-stop friction increase*. It is mainly correlated to the formation and shape adaptation of the contact plateaus and can be difficult to separate from effects related to increased temperature. During longer tests, however, it can be shown that the increase is independent of starting temperature, see Fig. 24. Despite the different starting temperatures, the stops start at an equal friction level.

A part of the increase is explained by the speed reduction during the stop. Most pads show a slightly higher friction at low sliding speeds. Still, the effect can be seen, but slightly reduced, when braking with constant speed, see Fig 25.

The magnitude of the in-stop friction increase is pad specific. Furthermore, it depends on the relative air humidity, as shown in Paper V. At high humidity, typically above 60 %RH, the in-stop increase is lower than in dry air.

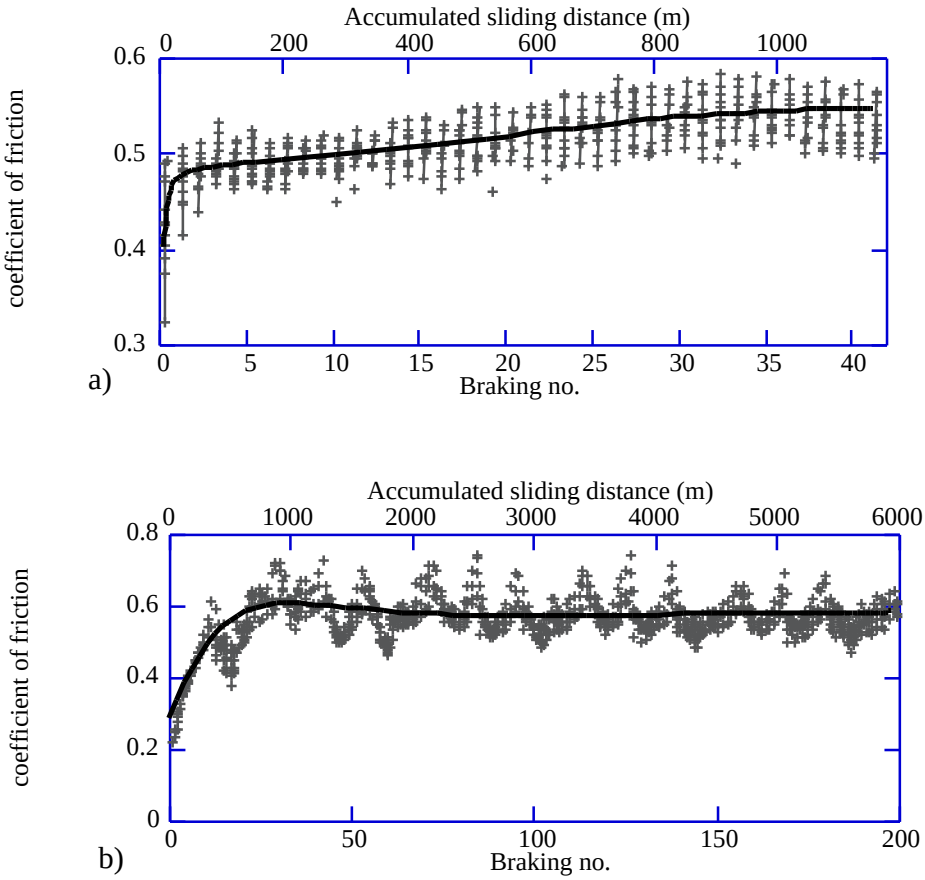

Fig. 23. Typical friction increase during run-in. The solid line indicates the average friction level and the grey pluses indicate individual friction measurements. Note the different x-axis scales.
a) Pad run-in, data points corresponding to one stop are connected with a grey line. (Pad material: MD 611B), b) Disc run-in. (Pad material: TX 4005)

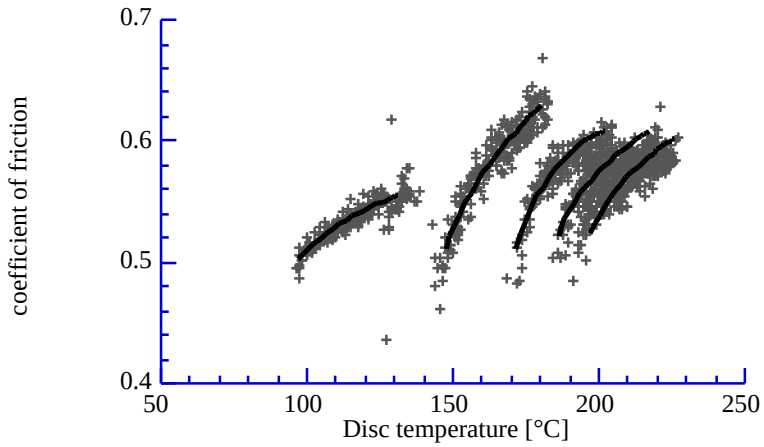

Fig. 24. In-stop friction increase for TX 4005 as a function of temperature. Note the equal starting friction level for the five stops, despite different starting temperatures.

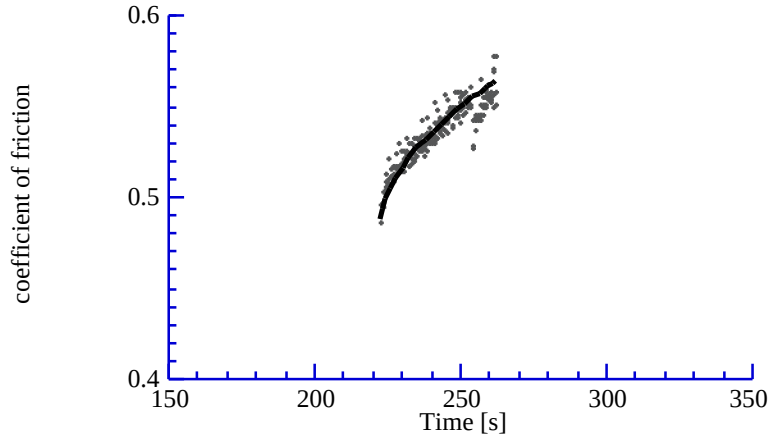

Fig. 25. In-stop friction increase of for TX 4005 while braking at constant pressure and sliding speed.

Friction hysteresis

The friction hysteresis is phenomenon first observed in Paper IV and further studied in Paper VI. The slow processes for contact area variations, such as formation and degradation of secondary plateaus, will cause a slow response in the coefficient of friction to pressure variations. When the pressure is increased, larger secondary plateaus are slowly formed. This growth will not be quick enough to allow a rapid increase and the ratio between elastic and plastic deformation of the plateaus will be shifted towards

plastic contact. As a result, the coefficient of friction will be slightly lower during increasing load than at constant or decreasing load. The opposite situation occurs for decreasing loads, where, at each load, the secondary plateaus will be slightly larger than for the same load held constant. This results in a more elastic contact and a higher coefficient of friction for braking with decreasing pressure.

Different pads have different plateau formation behaviour. Therefore, they also show different hysteresis behaviour. In Paper VI, it was observed that pads with a more pronounced plateau surface morphology displayed a larger friction hysteresis, see Fig 26.

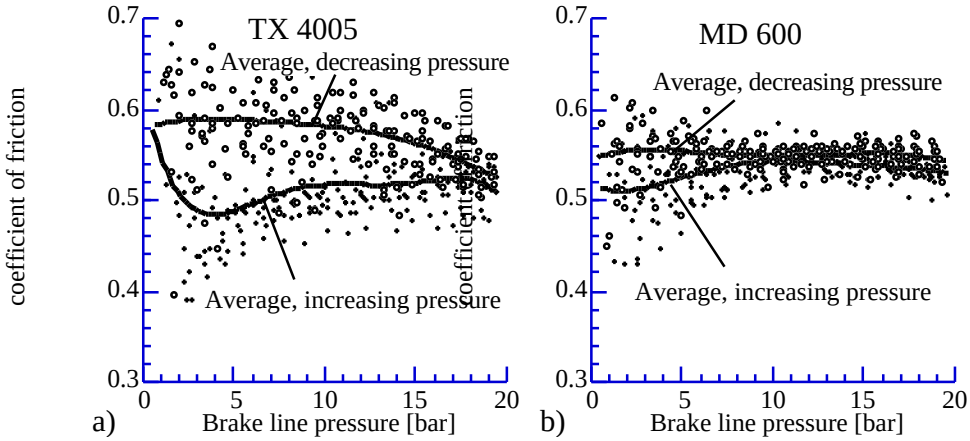

Fig. 26. Friction hysteresis for two different pad materials. Solid lines indicate the average friction level over five different brakings, all at a constant speed of 2 rps. Individual friction measurements are indicated with pluses and circles for increasing and decreasing brake pressure, respectively. Only every fifth data point is plotted. a) TX 4005, b) MD 600

4.2 Influence of humidity on the coefficient of friction.

In Paper V, the correlation between air humidity and the coefficient of friction, and also the squeal generation, was evaluated. It was concluded that all the tested pads showed a stable friction between 20 and 60 %RH. At elevated humidity, however, the pads displayed different behaviours. For two of the pads, the coefficient of friction was considerably lower and for one pad the friction was higher, see Fig. 27. The different behaviours are believed to be associated to the formation of tribofilms on the pad surfaces. More wear debris was gathered at low humidity than at high.

Furthermore, the in-stop friction increase was, generally, higher at low humidity. High relative humidity gave a stabilising effect on the friction.

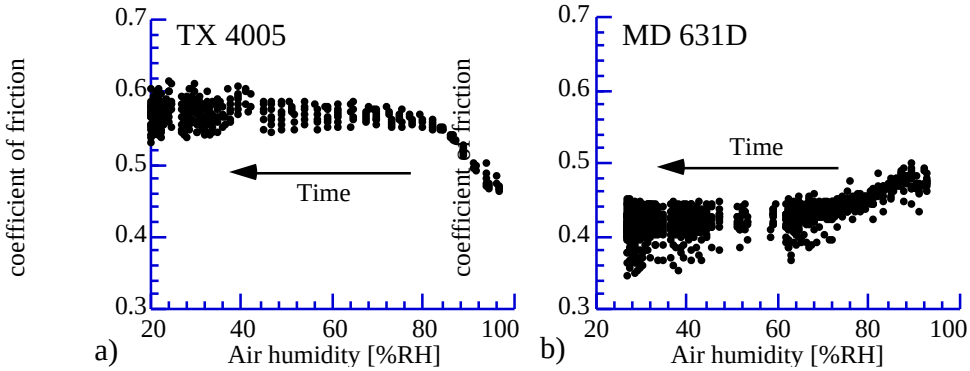

Fig. 27. Coefficient of friction versus relative air humidity for two different brake pads. Measured during decreasing air humidity. Paper V
a) TX 4005, b) MD 631D (MD 600 with 8 vol% Cu_2S added)

4.3 Correlation between μ and brake squeal

In the search for the mechanisms responsible for brake squeal generation, it is natural to study the friction behaviour of the brake. The friction force is the only mechanism supplying power to the system and is thus the driving force for squeal.

Squeal threshold

A general opinion within industry is that pads with high coefficient of friction are more prone to generate squeal than pads with low. This was also confirmed in Paper II and VI. Furthermore, these investigations demonstrated the existence of a squeal threshold in the coefficient of friction, below which no squeal is generated. In the present brake assembly, this threshold was found to be μ=0.4, see Fig. 28. A previous investigation by Bergman also indicated a similar level, in the same brake set-up [12]. Other brake assemblies probably show different squeal thresholds, as a result of different mechanical properties and designs. Nevertheless, the threshold behaviour is believed to be generally valid for all brake designs.

In figure 28b, it can further be seen that many data points above μ=0.4 corresponds to measurements during which no squeal was generated. A friction level above the threshold value is thus a necessary but not a sufficient condition for squeal to be generated.

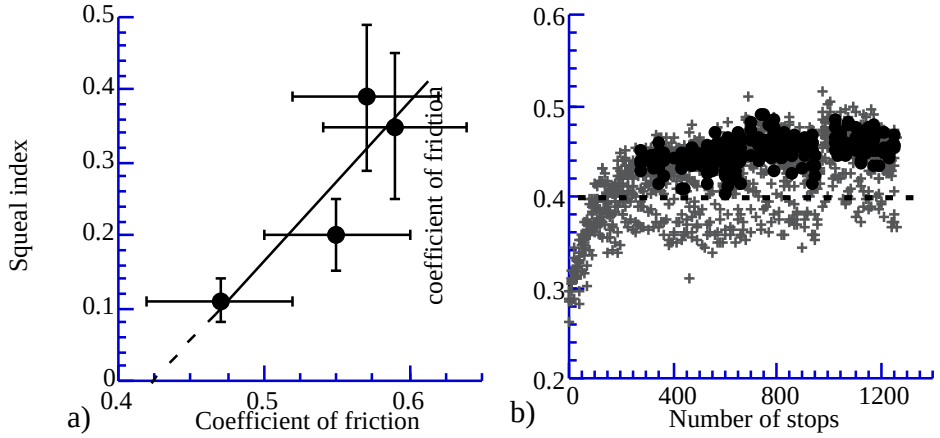

Fig. 28. Squeal generation and coefficient of friction in two different tests.
a) Squeal index versus average coefficient of friction for four different pads. For a pad with μ=0.4 no squeals would occur. (Paper VI)
b) Coefficient of friction during the run-in of a grit-blasted disc. Grey pluses indicate single friction measurements. The solid black circles indicate those friction values that were measured during squeal. No squeals were generated below μ=0.4. (Paper II)

Negative μ-velocity relation

A negative μ-velocity relation, $d\mu/dv<0$, or a higher static than dynamic friction coefficient was one of the first friction characteristics identified as increasing the squeal propensity [13, 14]. If the static friction is higher than the dynamic, stick-slip may occur between the rubbing surfaces [15].

The effect of different friction-velocity behaviours was studied in Paper VI. A number of different brake pads were evaluated with respect to friction behaviour with changing speed. The test was tailored to minimise the influence of temperature and run-in on the coefficient of friction. Three of the pads revealed a negative friction-velocity behaviour, see Fig. 29, but no correlation to squeal generation could be seen.

Influence of the normal load on the coefficient of friction

Over the last 15 years, finite element modelling (FEM) of different mechanical structures has become more easily accessible. From FEM modelling, it has been shown theoretically that squeal can be generated without a negative friction-velocity relation and that a high friction itself promotes squeal [11, 16, 17]. This correlates well with the experimental results in Paper II and VI.

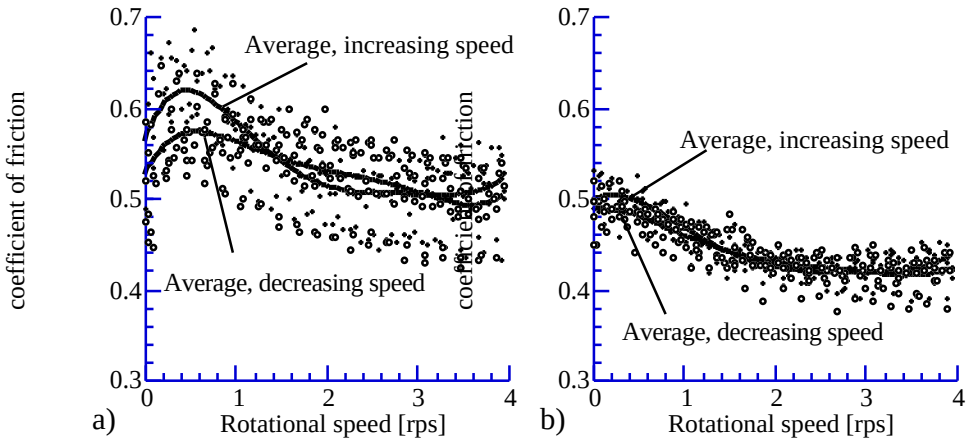

Fig. 29. Negative friction-velocity behaviour for two different pads. Evaluated under continuously changing speed, in order to minimise temperature and run-in effects. Individual friction measurements are indicated with pluses and circles for increasing and decreasing brake pressure, respectively.
a) Pad material showing high squeal index, MD 600.
b) Pad material showing low squeal index, MD 631D

In another FEM-study, Nagy predicted that squeal is more likely if the pad shows a positive friction-pressure behaviour, $d\mu/dp>0$ [18]. Experimentally, the correlation between different friction-load behaviours and squeal generation was investigated in Paper VI. Two of the pads showed friction hysteresis, described earlier, and a slight decrease in the coefficient of friction with increasing pressure. The other two pads showed a constant coefficient of friction over the investigated pressure range. Both behaviours are illustrated in Fig. 26.

No correlation was found between the different friction-load behaviours, or friction hysteresis, and squeal generation. This does not necessary indicate that no such correlation exists. The investigated behaviour is on a slower timescale than the mechanisms active in a brake squeal. A brake squeal with a frequency of 10 kHz causes a normal load redistribution over the pad with the same frequency. Thus, in order to get a squeal relevant friction characterisation, the measurements must be performed on the 0.1 ms timescale.

Furthermore, a sufficient lateral resolution is required. The pads bend during a squeal and due to the bending, the load is shifted between different areas of the pad surface. In order to measure the squeal related friction characteristics, not only the average over the whole surface, a lateral resolution higher than the bending shapes of the pad is needed.

4.4 Critical contact conditions

Despite the so-far unsuccessful attempts to find a clear correlation between different friction behaviours and squeal, a number of observations indicate that that the surface conditions really play a vital role for the generation of brake squeal. Some examples are outlined below:

Rapid onset and inhibition

In Paper III, it was shown that as soon as the surface conditions promote squeal, the onset is certain and rapid (<0.1s). In the short time within which the squeal started, nothing had changed but the surface conditions. When the conditions stopped promoting squeal, the inhibition was as quick as the onset, due to the effective damping of the system.

This was determined by a technique where a sector of the rubbing disc surface was prepared not to generate squeal. This "silent sector" was achieved by grit-blasting a sector of the disc surface, just as for the whole disc in Paper II. Now, during brakings when squeal was generated as the pad rubbed against the untreated disc surface, it immediately turned silent when rubbing against the sector. The squeal stopped as soon as the pad entered over the treated sector. Immediately after leaving the sector, and hence the surface conditions promoted squeal again, the squeal started.

Stochastic squeal behaviour

Another observation indicating that the surface conditions have a major influence on brake squeal, is the apparently stochastic behaviour of the squeal generation. Even in carefully controlled tests, with nominally identical conditions of pressure, temperature, humidity, history, etc, sometimes squeal occurs and sometimes it does not. The very small changes of the contact conditions during a test can lead to a transfer from silent to squealing conditions. These changes are so subtle that they are not easily measured or observed. The macro mechanical conditions, such as stiffness, hardness and design, do not have to change to transfer the brake from silence to squeal. Thus, the squeal appears to have a random behaviour, so that the onset of squeal under certain nominal conditions cannot be predicted, but described as a probability, only.

The only properties changing rapidly and unpredictably enough to give this seemingly random behaviour, are the surface conditions and the friction properties. In Paper VII, the rapid changes on the surface were observed. The contact conditions over a limited area of the pad changed completely within a second.

The presently applied evaluation methods, including calculation of the squeal index, has proven a powerful tool for evaluation of the squeal propensity of a brake system.

Taken together, these observations clearly indicate that studies of the contact conditions are necessary for an increased understanding of the squeal mechanisms in automotive brake systems.

5 SUMMARY

Disc brake squeal is just your ordinary every day problem. Yet, the friction mechanisms responsible are very subtle and difficult to study. In the present work, however, some observations and conclusions have been made:

No squeal is generated when the coefficient of friction is below a certain critical level, the squeal threshold. The level of the threshold depends on the design of the brake system, the material parameters and the friction characteristics.

Above this threshold, however, brake squeal is not certain. During a given set of conditions, there is only a probability for a squeal to be generated. Below the threshold, the probability is zero. Squeal generation in brake system is thus well described by the squeal index.

Despite constant nominal test conditions, the brake system can shift from silent to squealing behaviour. Variations in the contact situation on the micro level, is the only mechanism rapid and subtle enough to cause this shift, giving the brake its apparently stochastic squeal behaviour.

Nevertheless, as soon as the contact conditions promote squeal, the onset is certain and rapid (<0.1 s). When the conditions cease to promote squeal, the inhibition is as rapid, due to the effective damping of the system.

Studies of the friction behaviour are necessary to increase the understanding of the squeal phenomenon. This information is a vital ingredient in any model of the brake system, aiming at explaining the squeal behaviour.

Brake squeal is associated with a bending oscillation of the pads. A brake squeal with a frequency of 10 kHz causes a normal load redistribution over the pad surface with the same frequency as the squeal itself. In order to study squeal related friction behaviour, the measurements have to be performed on a timescale similar to that of the squeal itself. Thus, measurements of the friction characteristics must be performed, not only on the 0.1 ms timescale, but also with a sufficient lateral resolution. The required lateral resolution depends on the mode shape of the pad during squeal.

The friction behaviour of organic brake pads is closely related to the formation of *Contact plateaus* on the surface during braking. The number plateaus formed on an organic brake pad is on the order of 10^5. The plateau area can be subdivided into *the primary* and *secondary plateau.*

The primary plateaus are constituted by the wear resistant components of the pad and act as a nucleation sites for the secondary plateaus.

The secondary plateaus are formed by wear debris, compacted by the normal and frictional loads against the mechanically stable primary plateaus. Within a thin layer on top of the secondary plateaus, the debris is very well densified and sintered forming a homogenous material, a tribofilm. This tribofilm has a hardness close to that of the structural fibres. The rest of the secondary plateau, underneath the densified layer, is much softer.

The compliant nature of the pad helps distributing the load evenly over the contact areas (plateaus). Thanks to the low modulus of the matrix material, limiting the maximum load on each plateau, a very large number of plateaus can be in contact with the disc. The situation differs significantly from the contact occurring between two metal surfaces, where the high stiffness of the materials results in high pressures within a relatively small number of contact areas.

Formation and deterioration of the contact plateaus are important mechanisms, influencing the friction between the pad and the disc. Formation and shape adaptation of the plateaus are believed to explain some of the friction characteristics observed for organic brake pads, including in-stop, disc run-in and pad run-in friction increases, friction hysteresis and the reduced friction seen for a brake disc with small surface defects.

The presented contact situation, between an organic brake pad and solid cast iron disc, is unique for the given material combination and is so far undocumented in the literature.

6 ACKNOWLEDGEMENTS

This work has been carried out at the Tribomaterials Group, The Ångström Laboratory, Uppsala University. It has been financed by the Swedish National Board for Industrial and Technical Development. The project is a co-operation between Volvo AB and Uppsala University.

I am also grateful for the interesting and valuable discussions with, and material supply from, different friction material manufacturers, including A/S Roulunds Fabriker, Textar GmbH and AlliedSignal Inc.

Furthermore, I want to thank all my colleagues at the Materials Science Division for keeping up that ever so important friendly atmosphere. Especially, those keeping the technical and administrative machinery working: Rein, Janne, Carin and Ann-Sofie.

I also very much would like to thank:

Prof. Sture Hogmark for giving me the opportunity to work at the Tribomaterials Group. Hopefully, I will be able to beat him in Vasaloppet some day.

Prof. Staffan Jacobson, my supervisor, for helping me with all writing, except this section, and for making those smart and non-obvious conclusions. As I discovered during one of our brake escapades around the world, he also has a hidden talent for golf. You really ought to pick it up some day Staffan!

Dr. Filip Bergman, my co-worker during the first three years, for helping me and for sharing my interest for stupid facts and figures.

Mr. Claes Kuylenstierna, the project manager at Volvo Technological Development, for being so humble towards the subject and for being such a happy fellow.

Urban Simu and Henrik Björkman, for making the days at Ångström much more fun.

Kalle, among other things, for making that lovely illustration on page 11.

My dear family, especially Dad, Thomas and May, for their love and support and for inspiring me to start a career as a technician and a researcher. I also want to express my gratitude to my mother, for loving me and for always being a part of my memory.

Last, but not least, my beloved Maria, for all support and love and for being my best friend and, most importantly, for starting a PhD-career in Uppsala, without which we never would have met.

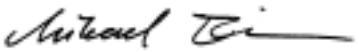

Mikael Eriksson, Uppsala, March 2000

7 REFERENCES

[1] H. Ford, Homepage of the Henry Ford Museum and Greenfield Village, 2000.

[2] D. Dowson, History of Tribology. second ed, 1998, Bury St Edmunds, Suffolk, Professional Engineering Publishing, 768.

[3] S. Jacobson and S. Hogmark, Tribologi. Karlebo-serien, 1996, Liber Utbildning. (Text book in Swedish)

[4] H. Smales, Friction materials - black art or science? Proceedings of the Institution of Mechanical Engineers, Part D: Journal of Automobile Engineering, 1995, 209(3), p. 151-157.

[5] H.P. Wallin, *et al.*, Ljud och Vibrationer, ed. M.W. Laboratory, 1999, Kongl. Tekniska Högskolan. (Text book in Swedish)

[6] J. Fieldhouse, A proposal to predict the noise frequency of a disc brake based on friction pair interface geometry, in 17th Annual brake colloquium and engineering display, 1999, Miami Beach, FL, USA, SAE Paper 1999-01-3403.

[7] M. Eriksson, Belägg med hårda kontaktfläckar ger bromsskrik - friktionsfilm saknas på skivorna, in Secondary, , M. Eriksson, 1996, Materialvetenskap, Uppsala, UPTEC 96 035E. (Masters thesis in Swedish)

[8] M.G. Jacko, P.H.S. Tsang, and S.K. Rhee, Wear debris compaction and friction film formation of polymer composites, in International Conference on Wear of Materials, 1989, p. 469-480.

[9] F. Bergman, M. Eriksson, and S. Jacobson, The effect of reduced contact area on the occurrence of brake squeals for an automotive brake pad. Submitted to Journal of Automobile Engineering, 1999.

[10] J. Hultén, Drum Brake Squeal - A Self-Exciting Mechanism with Constant Friction, in SAE Truck and Bus Meeting, 1993, Detroit, Michigan, USA, SAE Paper 93 29 65.

[11] J. Hultén, Friction Phenomena Related to Drum Brake Squeal Instabilities, in ASME Design Engineering Technical Conferences, 1997, Sacramento, California, ASME Paper DETC97/VIB-4161.

[12] F. Bergman, M. Eriksson, and S. Jacobson, The effect of Cu_2S solid lubricant addition, and varying density, on the occurrence of brake squeals for one low-metal, organic type friction material, in The 17:th Annual SAE Brake Colloquium & Engineering Display, 1999, Miami Beach, Miami, SAE Paper 1999-01-3394

[13] R.A.C. Fosberry and Z. Holubecki, Interim Report on Disc Brake Squeal. M. I. R. A, 1959, 1959/4.

[14] R.A.C. Fosberry and Z. Holubecki, Disc brake squeal; its mechanisms and suppression. M.I.R.A Research Report, 1961, 1961/2.

[15] E. Rabinowicz, Friction fluctuations, in Fundamentals of Friction: Macroscopic and Microscopic Processes, I.L. Singer and H.M. Pollock, 1992, Kluver Academic Publishers. p. 25-34.

[16] M.L. Chargin, L.W. Dunne, and D.N. Herting, Nonlinear dynamics of brake squeal. Finite element analysis and design, 1997, 28, p. 69-82.

[17] G.D. Liles, Analysis of Disc Brake Squeal Using Finite Element Methods. SAE Technical paper series, 1998, p. Paper no. 891150.

[18] L.I. Nagy, J. Cheng, and Y.-K. Hu, A new method development to predict brake squeal occurence. SAE transactions, 1994, 103, p. 416-423.